

Structural instability and charge modulations in the Kagome superconductor AV_3Sb_5

Zijin Ye,¹ Aiyun Luo,¹ Jia-Xin Yin,² M Zahid Hasan,² and Gang Xu^{1,*}

¹Wuhan National High Magnetic Field Center and School of Physics,
Huazhong University of Science and Technology, Wuhan 430074, China

²Laboratory for Topological Quantum Matter and Advanced Spectroscopy (B7),
Department of Physics, Princeton University, Princeton, New Jersey 08544, USA
(Dated: November 16, 2021)

Recently, both charge density wave (CDW) and superconductivity have been observed in Kagome compounds AV_3Sb_5 . However, the nature of CDW that results in many novel charge modulations is still under hot debate. By means of the first-principles calculations, we discover two kinds of CDW states, the trimerized and hexamerized 2×2 phase and dimerized 4×1 phase existing in AV_3Sb_5 . Our phonon excitation spectrum and electronic Lindhard function calculations reveal that the most intensive structural instability in AV_3Sb_5 originates from a combined in-plane vibration mode of V atoms through the electron-phonon coupling, rather than the Fermi surface nesting effect. Crucially, a metastable 4×1 phase with V-V dimer pattern and twofold symmetric bowtie shaped charge modulation is revealed in CsV_3Sb_5 , implying that both dimerization and trimerization exist in the V Kagome layers. These results provide essential understanding of CDW instability and new thoughts for the novel charge modulation patterns.

Kagome materials are the unique platform to study the topological physics [1], flat band [2], geometrical spin frustration [3] and their interactions. At the beginning, large band gap Kagome magnets are widely studied as the promising quantum spin liquid system [4–8]. Encouraged by the quantum anomalous Hall (QAH) effect proposed in the ferromagnetic Kagome material $Cs_2LiMn_3F_{12}$ [1], the topological physics [9–11], electronic correlated flat band [2, 12] and quantum transport induced by the nontrivial Berry curvature [13, 14] in the Kagome metals have attracted increasing interest. Additionally, the interplay between electronic correlation, magnetic frustration and topology usually gives rise to a variety of intriguing quantum phenomena [15], such as fractional QAH effect [16], topological phase transition [17], spin or charge density waves (SDWs or CDWs) [18, 19] and superconductivity [20–22]. Recently, a new family of quasi-two-dimensional (quasi-2D) Kagome metal AV_3Sb_5 ($A = K, Rb, Cs$) has been synthesized [23], and reported to host nontrivial topological bands [24], unconventional superconductivity [25, 26], van Hove singularities (VHS) and CDW [27–31], which provide a natural platform to study the interplay between these quantum states.

As shown in Fig. 1(a), the pristine AV_3Sb_5 compounds share same layered structure satisfying space group $P6/mmm$ (No. 191), where A atoms at $1a$ (0, 0, 0) site form the triangle lattice, V atoms at $3g$ ($\frac{1}{2}$, 0, $\frac{1}{2}$) site form a Kagome layer, Sb1 atoms at $1b$ (0, 0, $\frac{1}{2}$) occupy the center of V hexagon and Sb2 atoms at $4h$ ($\frac{1}{3}$, $\frac{2}{3}$, z) form two honeycomb layers. These materials undergo a CDW transition as cooling down to about 80 - 100 K [25, 27, 28], and enter to the superconducting phase with $T_c = 0.9 - 2.5$ K [25, 26, 32]. For the CDW phase, a 2×2 or $2\times 2\times 2$ superlattice with trimerization and hexamerization of V atoms (referred to as T&H

phase) is discovered in KV_3Sb_5 [27] and CsV_3Sb_5 [29, 34]. Very recently, an additional 4×1 CDW phase is further observed by scanning tunneling microscopy (STM) experiments in CsV_3Sb_5 when the samples are cooled down to 50 K [35, 51, 52]. Some theoretical and experimental works suggested that the CDW might be originated from the electron correlation [19, 36–44]. Some X-ray scattering and angle-resolved photoemission spectroscopy (ARPES) experiments suggest that it is purely induced by the Fermi surface (FS) nesting of the VHS at M points [45]. Besides, recent ARPES and neutron scattering experiments propose that the 2×2 CDW phase in AV_3Sb_5 is mainly driven by the electron-phonon coupling (EPC) [46–50]. For the 4×1 CDW, Zhao *et al.* propose that it may be associated with the bulk electronic nematicity [51, 52], while Li *et al.* attribute it to the surface instability and electron correlation [53]. Therefore, the nature of CDW and its relation to the electronic structures, EPC, electron correlation and superconductivity remain under hot debate in AV_3Sb_5 .

In this paper, we construct a variety of supercells to study the structural instability and charge modulation in AV_3Sb_5 based on the first-principles calculations. Our calculations reveal that the most stable structure in AV_3Sb_5 is the 2×2 T&H phase, and the reconstruction along c -direction is negligible. Further phonon spectrum and Lindhard function calculations demonstrate that such CDW instability is mainly driven by a combined in-plane vibration mode of V atoms, rather than the FS nesting effect. Such vibration gives rise to a negative phonon mode at M point, which can be hardened after the trimerization and hexamerization of V atoms in the T&H phase. More importantly, a metastable 4×1 phase with V-V dimer pattern is also discovered in CsV_3Sb_5 , leading to a twofold symmetric bowtie shaped charge modulation that has never been observed previously. The

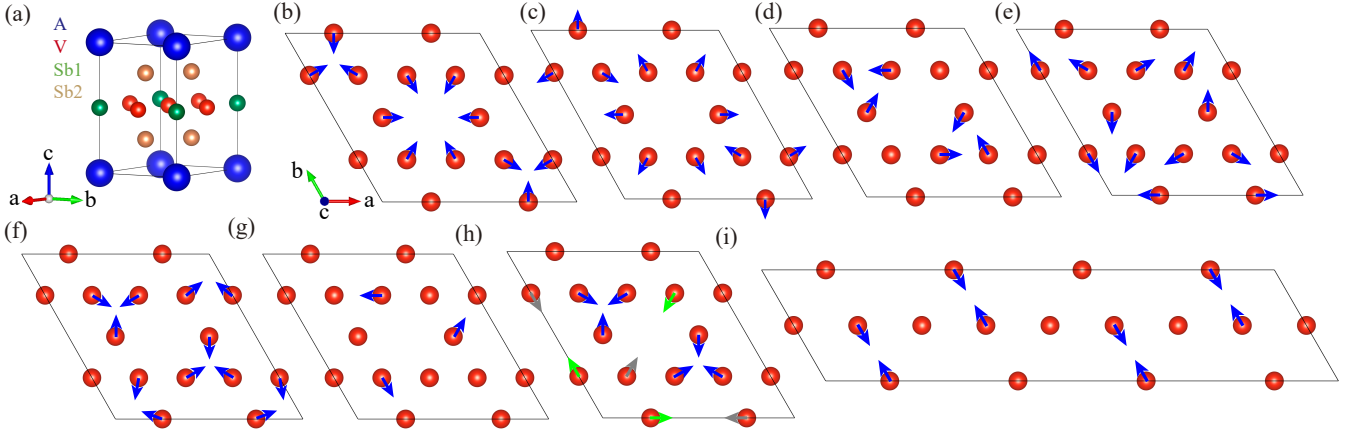


FIG. 1. (a) The crystal structure of pristine AV_3Sb_5 . (b)-(i) The top view along the c -axis of V Kagome layer in the 2×2 supercells satisfying D_{6h} ((b) for T&H, (c) for DS), C_{6h} (d), D_{3d} (e), D_{3h} (f), C_{3h} (g), C_{3v} (h) and 4×1 Dimer phase (i), respectively. The blue arrows represent pure in-plane movements, and the green (gray) arrows represent in-plane movements with a slight upward (downward) shift along c direction.

TABLE I. The energy of KV_3Sb_5 in different structures.

Structure	Energy (eV/f.u.)
pristine	-50.511
T&H	-50.519
DS	-50.514
C_{6h}	-50.518
D_{3d}	-50.514
D_{3h}	-50.518
C_{3h}	-50.514
C_{3v}	-50.514

TABLE II. The energy of CsV_3Sb_5 in different structures.

Structure	Energy (eV/f.u.)	
pristine	-50.571	
	(2×2) $(2 \times 2 \times 2)$	
T&H	-50.586	-50.586
C_{6h}	-50.585	-50.585
D_{3d}	-50.575	-50.575
C_{3v}	-50.575	-50.575
4×1 Dimer	-50.574	
$4 \times 1 \times 2$ Dimer	-50.574	

bowtie shaped charge modulation may be responsible to the twofold resistivity anisotropy in CsV_3Sb_5 [52]. Our results demonstrate that the competition between dimerization and trimerization may exist in CsV_3Sb_5 , which shed lights on the essential understanding of CDW instability and other novel phenomena.

Our first-principles calculations are carried out by the Vienna ab initio simulation package (VASP) [55–57]. The generalized gradient approximation (GGA) of the Perdew-Burke-Ernzerhof (PBE) type is adopted for the exchange-correlation potential [58]. The cut-off energy for the wave function expansion is set to 500 eV and $16 \times 16 \times 9$ k-mesh is used to sample the first Brillouin zone (BZ). The experimental lattice parameters $a = 5.482 \text{ \AA}$, $c = 8.958 \text{ \AA}$ for KV_3Sb_5 and $a = 5.44 \text{ \AA}$, $c = 9.33 \text{ \AA}$ for CsV_3Sb_5 are used [29], and all structures are optimized until the force on each atom is less than 0.01 eV/\AA . The unfolded band structures of CsV_3Sb_5 are obtained from the Wannier functions by using WANNIER90 [59] and WannierTools package [60].

Considering that many experimental results indicate the time reversal symmetry breaking in AV_3Sb_5 [24, 27, 33, 54, 61–63], we study their magnetic instability by cal-

culating many magnetic configurations. However, their energies always return to that of non-magnetic (NM) state [SM], indicating that any magnetism has not been found in the Density Functional Theory level. These results are consistent with recent experiments [23, 64], implying that time reversal symmetry breaking effect may come from CDW transition or electron correlation.

According to the above calculations, we will study the structural instability of AV_3Sb_5 just based on the NM calculations for different supercells and structural distortions. First, let us focus on the structural instability of KV_3Sb_5 . For this purpose, we construct a 2×2 supercell from the pristine phase, and lower its symmetry by adjusting the coordinates of V atoms. As a result, seven structural configurations as shown in Fig. 1(b)-(h) are obtained. We notice that the T&H phase in Fig. 1(b) and David star (DS) phase in Fig. 1(c) both satisfy the point group D_{6h} , and Figs. 1(d)-(h) satisfy C_{6h} , D_{3d} , D_{3h} , C_{3h} and C_{3v} point group, respectively. In order to find the most stable structure, all the above superlattices and also the pristine structure of KV_3Sb_5 are optimized. The calculated energies are listed in TABLE I. It demonstrates that the T&H phase with the shrunk

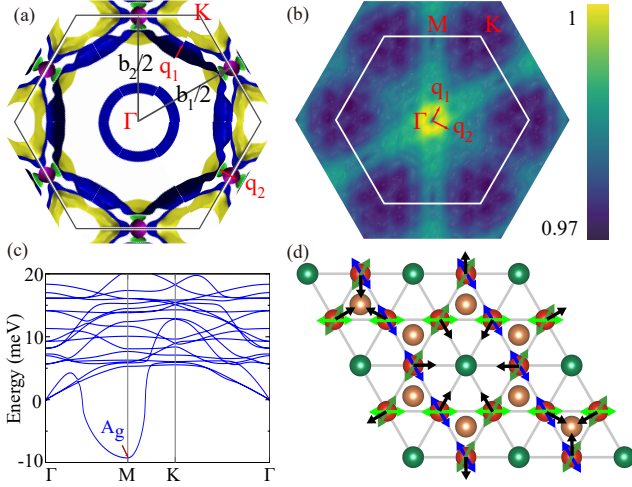


FIG. 2. (a) The top view of the FSs of KV_3Sb_5 along the (001) direction. Two red arrows represent two small nesting vectors \vec{q}_1 and \vec{q}_2 . (b) Normalized 2D Lindhard response function $\chi_0(q)$ in the b_1 - b_2 plane. (c) The phonon spectrum of pristine CsV_3Sb_5 . (d) The A_g vibration modes of V atoms at three M points. The blue, orange and green arrows represent the vibration at M_1 ($\pi, 0, 0$), M_2 ($0, \pi, 0$) and M_3 ($\pi, \pi, 0$) points, respectively. The black arrows respect the total vibration direction.

trimers and hexamers of the V atoms is the most stable one, which well agrees with previous experiments and calculations [27, 29]. Further analysis shows that, after the optimization, the V atoms in many other structures tend to the same movements as that in T&H phase. These results indicate that the trimerization and hexamerization of V atoms play important roles to stabilize the crystal structure in AV_3Sb_5 .

Very similar results and conclusions are obtained in the 2×2 superlattice of CsV_3Sb_5 . We select T&H phase, C_{6h} , D_{3d} and C_{3v} type of structures as representatives and list the calculated results in TABLE II. Furthermore, starting from the 2×2 structures, we also construct the corresponding $2 \times 2 \times 2$ structural configurations by modulating the V atoms along c -direction. The calculated energies of the optimized $2 \times 2 \times 2$ structures are the same as that of the corresponding 2×2 structures, as shown in TABLE II. Therefore, we conclude that the energy change caused by the c -direction reconstruction is negligible, indicating that the CDW in AV_3Sb_5 is mainly come from the in-plane instability.

Besides, a metastable 4×1 supercell satisfying C_{2h} point group symmetry is also discovered for the bulk and film calculations of CsV_3Sb_5 , which corresponds to the experimental observations well [35, 51, 52]. As shown in TABLE II, the energy of such 4×1 supercell is 3 meV/f.u. lower than the pristine phase and 12 meV/f.u. higher than the T&H phase. More detailed analysis reveals that a dimer pattern along (010) direction, rather than the trimers and hexamers in 2×2 superlattice, is formed in

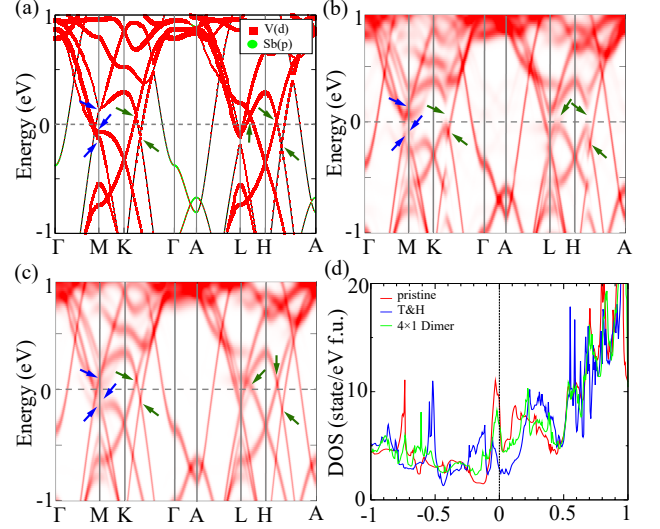


FIG. 3. (a) The projected band structures of pristine CsV_3Sb_5 . (b)-(c) The unfolded band structures of 2×2 T&H phase and 4×1 Dimer phase, respectively. The blue and dark green arrows indicate VHS points and Dirac points, respectively. (d) The DOS of CsV_3Sb_5 in pristine phase (red), 2×2 T&H phase (blue) and 4×1 Dimer phase (green).

such 4×1 supercell, as shown in Fig. 1(i). Moreover, a $4 \times 1 \times 2$ supercell is constructed but failed to search for other kind of structural configuration. It always gives rise to the same energy and atomic modulation pattern as in the 4×1 supercell, which further demonstrates that the in-plane instability is the main driven force of the CDW in AV_3Sb_5 .

In order to check whether the CDW instability originates from the FS nesting and the Peierls instability as pointed out by the recent X-ray scattering and ARPES experiments [45], we calculate the FSs of the pristine KV_3Sb_5 and plot top view of them in Fig. 2(a). The FSs of KV_3Sb_5 have quasi-2D characteristics with a columnar FS around Γ center, while another tri-prismatic FSs surround K point. As a result, the FSs do not show any overlap by shifting them of vector $\vec{b}_1/2$ or $\vec{b}_2/2$, and only weak FS nesting effect can be induced by shifting two small vectors, \vec{q}_1 and \vec{q}_2 , as shown in Fig. 2(a). Lindhard response function $\chi_0(q)$ is a straightforward evidence to reflect the FS nesting instability [65]. We calculate the 2D renormalized $\chi_0(q)$ of KV_3Sb_5 and plot it in Fig. 2(b). Obviously, no peaks of $\chi_0(q)$ appear at the nesting vectors $\vec{b}_1/2$ or $\vec{b}_2/2$ that correspond to the 2×2 supercell. Fig. 2(b) just exhibits some weak peaks at small \vec{q} , i.e., \vec{q}_1 and \vec{q}_2 in Fig. 2(a). These results strongly demonstrate that the CDW instability in AV_3Sb_5 is not from the FS nesting effect.

Next, we focus our attention on the phonon spectrum of AV_3Sb_5 , and display the results of CsV_3Sb_5 to study the structural instability induced by EPC. The calculated phonon spectrum of pristine CsV_3Sb_5 is plotted in

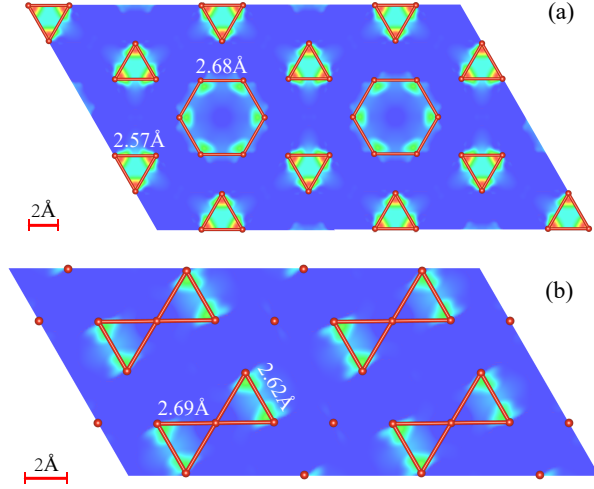


FIG. 4. (a)-(b) The differential charge density distribution in V Kagome layer of CsV_3Sb_5 in 2×2 T&H phase and 4×1 Dimer phase, respectively.

Fig. 2(c). We clarify that the softening branch phonon shown at $M(\pi, 0, 0)$ point of Fig. 2(c) has A_g representation, which corresponds to the vibration mode of V atoms along (010) direction, as illustrated by the blue arrows in Fig. 2(d). Furthermore, the A_g mode at other two M points, i.e. $(0, \pi, 0)$ and $(\pi, \pi, 0)$, give rise to the vibration of V atoms along (100) and (110) direction, respectively. Combining the A_g modes at three M points, the total vibration modes are consistent with movements of V atoms in T&H or DS phase. In order to strengthen such softening mode, one natural manner is to shorten the distance between V atoms as occurred in the T&H phase (see the black arrows in Fig. 2(d)). Thus our results demonstrate that the EPC plays crucial roles in the formation of the 2×2 or $2\times 2\times 2$ CDW phase in AV_3Sb_5 , which is consistent with the very recent neutron scattering experiment [50] very well. On the other hand, the 4×1 instability seems more complex. Electron correlation and surface instability may need to be taken into account in order to well address this problem [35, 51, 52].

In the following, we would like to discuss the changes of the electronic properties between different structural phase. In Fig. 3(a), we plot the projected band structure of pristine CsV_3Sb_5 . Consistent with previous reports [23], there are many VHS points and Dirac points close to the Fermi level, resulting in a relatively high density of states (DOS) at Fermi level ($N_{E_f} = 8.92$ state/(eV f.u.)). After the 2×2 reconstruction, most of the VHS points and Dirac points are gapped as shown in Fig. 3(b), which leads to a DOS transformation from Fermi level to the higher or lower energy. We notice that, non-zero Berry curvature is usually associated with the gapped Dirac points [66], which may be the reason of the observed anomalous Hall effect [24, 33]. In the metastable

4×1 Dimer phase, only the spectra weight contributed by the VHS points at M point is weakened, while the Dirac points are marginally affected, as shown in Fig. 3(c). So that a weak DOS suppression is observed. We have summarized the change of DOS in Fig. 3(d), which demonstrates that the 2×2 and 4×1 reconstruction lead to different DOS suppression at Fermi level, and give rise to $N_{E_f} = 2.84$ state/(eV f.u.) for 2×2 T&H phase and $N_{E_f} = 6.93$ state/(eV f.u.) for 4×1 Dimer phase respectively.

Finally, we calculate the differential charge density distribution of 2×2 T&H and 4×1 Dimer CsV_3Sb_5 , i.e., the real space charge difference between the CDW phase and pristine phase, which reveals the real space charge modulation directly and can be compared with the STM observations qualitatively. The differential charge density distribution in V Kagome layer is plotted in Fig. 4. In the 2×2 T&H phase, the bonds of V trimers (2.57 Å) and hexamers (2.68 Å) are shorter than that of the pristine Kagome lattice (2.72 Å). Particularly, Fig. 4(a) illustrates that the charge density in the V trimers is higher than that in the V hexamers, indicating a stronger charge assembling effect in the trimer, which agree with previous experimental and theoretical results well [30]. On the other hand, the charge density modulation in 4×1 Dimer phase is quite different from that in the 2×2 T&H phase. As illustrated in Fig. 4(b), the V atoms in the 4×1 Dimer phase tend to form the V-V dimers along (010) direction with bond length 2.62 Å. These results indicate that there may exist the competition between dimerization and trimerization in CsV_3Sb_5 . More importantly, a twofold symmetric bowtie shaped charge accumulation emerges as shown in Fig. 4(b). Such totally new charge modulation has never been reported previously and may be responsible to the twofold resistivity anisotropy in CsV_3Sb_5 [52]. Lastly, we would like to notice that, the charge modulation in 4×1 phase is somewhat weaker than that in the 2×2 T&H phase, which is consistent with the analysis of their electronic structures in Fig. 3.

In summary, our results demonstrate that the most stable structure in AV_3Sb_5 is the 2×2 supercell with trimerization and hexamerization of V atoms. The phonon spectrum and Lindhard function calculations strongly suggest that such CDW phase is mainly driven by phonon instability through EPC instead of the FS nesting effect, which agree with many latest experimental observations very well [29, 30, 45, 54]. In particular, a metastable 4×1 phase with V-V dimer pattern is also discovered in CsV_3Sb_5 , in which a twofold symmetric bowtie shaped charge modulation is first reported and need further experimental confirmation.

We thanks the valuable discussion with JianZhou Zhao. This work is supported by the Ministry of Science and Technology of China (No. 2018YFA0307000) and the National Natural Science Foundation of China (No. 11874022). Work at Princeton University is supported by

the Gordon and Betty Moore Foundation (GBMF4547 and GBMF9461).

* gangxu@hust.edu.cn

- [1] G. Xu, B. Lian, and S.-C. Zhang, Intrinsic quantum anomalous hall effect in the kagome lattice $\text{Cs}_2\text{LiMn}_3\text{F}_{12}$, *Phys. Rev. Lett.* **115**, 186802 (2015).
- [2] J.-X. Yin, S. S. Zhang, G. Chang, Q. Wang, S. S. Tsirkin, Z. Guguchia, B. Lian, H. Zhou, K. Jiang, I. Belopolski, N. Shumiya, D. Multer, M. Litskevich, T. A. Cochran, H. Lin, Z. Wang, T. Neupert, S. Jia, H. Lei, and M. Z. Hasan, Negative flat band magnetism in a spin-orbit-coupled correlated kagome magnet, *Nature Physics* **15**, 443 (2019).
- [3] M. Norman, Colloquium: Herbertsmithite and the search for the quantum spin liquid, *Reviews of Modern Physics* **88**, 041002 (2016).
- [4] A. Olariu, P. Mendels, F. Bert, F. Duc, J. C. Trombe, M. A. de Vries, and A. Harrison, ^{17}O NMR study of the intrinsic magnetic susceptibility and spin dynamics of the quantum kagome antiferromagnet $\text{ZnCu}_3(\text{OH})_6\text{Cl}_2$, *Phys. Rev. Lett.* **100**, 087202 (2008).
- [5] L. Balents, Spin liquids in frustrated magnets, *Nature* **464**, 199 (2010).
- [6] S. Yan, D. A. Huse, and S. R. White, Spin-liquid ground state of the $s=1/2$ kagome Heisenberg antiferromagnet, *Science* **332**, 1173 (2011).
- [7] T.-H. Han, J. S. Helton, S. Chu, D. G. Nocera, J. A. Rodriguez-Rivera, C. Broholm, and Y. S. Lee, Fractionalized excitations in the spin-liquid state of a kagome-lattice antiferromagnet, *Nature* **492**, 406 (2012).
- [8] Y. Shen, Y.-D. Li, H. Wo, Y. Li, S. Shen, B. Pan, Q. Wang, H. Walker, P. Steffens, M. Boehm, *et al.*, Evidence for a spinon Fermi surface in a triangular-lattice quantum-spin-liquid candidate, *Nature* **540**, 559 (2016).
- [9] L. Ye, M. Kang, J. Liu, F. Von Cube, C. R. Wicker, T. Suzuki, C. Jozwiak, A. Bostwick, E. Rotenberg, D. C. Bell, *et al.*, Massive Dirac fermions in a ferromagnetic kagome metal, *Nature* **555**, 638 (2018).
- [10] J.-X. Yin, W. Ma, T. A. Cochran, X. Xu, S. S. Zhang, H.-J. Tien, N. Shumiya, G. Cheng, K. Jiang, B. Lian, *et al.*, Quantum-limit Chern topological magnetism in TbMn_6Sn_6 , *Nature* **583**, 533 (2020).
- [11] H. Tsai, T. Higo, K. Kondou, T. Nomoto, A. Sakai, A. Kobayashi, T. Nakano, K. Yakushiji, R. Arita, S. Miwa, *et al.*, Electrical manipulation of a topological antiferromagnetic state, *Nature* **580**, 608 (2020).
- [12] M. Kang, L. Ye, S. Fang, J.-S. You, A. Levitan, M. Han, J. I. Facio, C. Jozwiak, A. Bostwick, E. Rotenberg, *et al.*, Dirac fermions and flat bands in the ideal kagome metal FeSn , *Nature materials* **19**, 163 (2020).
- [13] S. Nakatsuji, N. Kiyohara, and T. Higo, Large anomalous hall effect in a non-collinear antiferromagnet at room temperature, *Nature* **527**, 212 (2015).
- [14] E. Liu, Y. Sun, N. Kumar, L. Muechler, A. Sun, L. Jiao, S.-Y. Yang, D. Liu, A. Liang, Q. Xu, *et al.*, Giant anomalous Hall effect in a ferromagnetic kagome-lattice semimetal, *Nature physics* **14**, 1125 (2018).
- [15] J.-X. Yin, S. S. Zhang, H. Li, K. Jiang, G. Chang, B. Zhang, B. Lian, C. Xiang, I. Belopolski, H. Zheng, *et al.*, Giant and anisotropic many-body spin-orbit tunability in a strongly correlated kagome magnet, *Nature* **562**, 91 (2018).
- [16] E. Tang, J.-W. Mei, and X.-G. Wen, High-temperature fractional quantum hall states, *Phys. Rev. Lett.* **106**, 236802 (2011).
- [17] Z. He, A. Luo, B. Lian, and G. Xu, Interplay of topological electrons and magnons in the kagome magnet $\text{CoCu}_3(\text{OH})_6\text{Cl}_2$, *Phys. Rev. B* **103**, 113007 (2021).
- [18] S.-L. Yu and J.-X. Li, Chiral superconducting phase and chiral spin-density-wave phase in a Hubbard model on the kagome lattice, *Phys. Rev. B* **85**, 144402 (2012).
- [19] W.-S. Wang, Z.-Z. Li, Y.-Y. Xiang, and Q.-H. Wang, Competing electronic orders on kagome lattices at van Hove filling, *Phys. Rev. B* **87**, 115135 (2013).
- [20] M. L. Kiesel and R. Thomale, Sublattice interference in the kagome Hubbard model, *Phys. Rev. B* **86**, 121105 (2012).
- [21] M. L. Kiesel, C. Platt, and R. Thomale, Unconventional fermi surface instabilities in the kagome hubbard model, *Phys. Rev. Lett.* **110**, 126405 (2013).
- [22] C. Mielke, Y. Qin, J.-X. Yin, H. Nakamura, D. Das, K. Guo, R. Khasanov, J. Chang, Z. Q. Wang, S. Jia, S. Nakatsuji, A. Amato, H. Luetkens, G. Xu, M. Z. Hasan, and Z. Guguchia, Nodeless kagome superconductivity in LaRu_3Si_2 , *Phys. Rev. Materials* **5**, 034803 (2021).
- [23] B. R. Ortiz, L. C. Gomes, J. R. Morey, M. Winiarski, M. Bordelon, J. S. Mangum, I. W. H. Oswald, J. A. Rodriguez-Rivera, J. R. Neilson, S. D. Wilson, E. Ertekin, T. M. McQueen, and E. S. Toberer, New kagome prototype materials: discovery of KV_3Sb_5 , RbV_3Sb_5 , and CsV_3Sb_5 , *Phys. Rev. Materials* **3**, 094407 (2019).
- [24] S.-Y. Yang, Y. Wang, B. R. Ortiz, D. Liu, J. Gayles, E. Derunova, R. Gonzalez-Hernandez, L. Šmejkal, Y. Chen, S. S. P. Parkin, S. D. Wilson, E. S. Toberer, T. McQueen, and M. N. Ali, Giant, unconventional anomalous Hall effect in the metallic frustrated magnet candidate, KV_3Sb_5 , *Science Advances* **6**, 10.1126/sciadv.abb6003 (2020).
- [25] B. R. Ortiz, S. M. L. Teicher, Y. Hu, J. L. Zuo, P. M. Sarte, E. C. Schueller, A. M. M. Abeykoon, M. J. Krogstad, S. Rosenkranz, R. Osborn, R. Seshadri, L. Balents, J. He, and S. D. Wilson, CsV_3Sb_5 : A \mathbb{Z}_2 topological kagome metal with a superconducting ground state, *Phys. Rev. Lett.* **125**, 247002 (2020).
- [26] Y. Wang, S. Yang, P. K. Sivakumar, B. R. Ortiz, S. M. L. Teicher, H. Wu, A. K. Srivastava, C. Garg, D. Liu, S. S. P. Parkin, E. S. Toberer, T. McQueen, S. D. Wilson, and M. N. Ali, Proximity-induced spin-triplet superconductivity and edge supercurrent in the topological kagome metal, $\text{K}_{1-x}\text{V}_3\text{Sb}_5$ (2020), [arXiv:2012.05898](https://arxiv.org/abs/2012.05898) [[cond-mat.supr-con](https://arxiv.org/archive/cond-mat)].
- [27] Y.-X. Jiang, J.-X. Yin, M. M. Denner, N. Shumiya, B. R. Ortiz, G. Xu, Z. Guguchia, J. He, M. S. Hossain, X. Liu, J. Ruff, L. Kautzsch, S. S. Zhang, G. Chang, I. Belopolski, Q. Zhang, T. A. Cochran, D. Multer, M. Litskevich, Z.-J. Cheng, X. P. Yang, Z. Wang, R. Thomale, T. Neupert, S. D. Wilson, and M. Z. Hasan, Unconventional chiral charge order in kagome superconductor KV_3Sb_5 , *Nature Materials* **20**, 1353 (2021).
- [28] Q. Yin, Z. Tu, C. Gong, Y. Fu, S. Yan, and H. Lei, Superconductivity and normal-state properties of kagome

- metal RbV₃Sb₅ single crystals, *Chinese Physics Letters* **38**, 037403 (2021).
- [29] H. Tan, Y. Liu, Z. Wang, and B. Yan, Charge density waves and electronic properties of superconducting kagome metals, *Phys. Rev. Lett.* **127**, 046401 (2021).
- [30] X. Feng, K. Jiang, Z. Wang, and J. Hu, Chiral flux phase in the kagome superconductor AV₃Sb₅, *Science Bulletin* **66**, 1384 (2021).
- [31] J. Zhao, W. Wu, Y. Wang, and S. A. Yang, Electronic correlations in the normal state of the kagome superconductor KV₃Sb₅, *Phys. Rev. B* **103**, L241117 (2021).
- [32] B. R. Ortiz, P. M. Sarte, E. M. Kenney, M. J. Graf, S. M. L. Teicher, R. Seshadri, and S. D. Wilson, Superconductivity in the \mathbb{Z}_2 kagome metal KV₃Sb₅, *Phys. Rev. Materials* **5**, 034801 (2021).
- [33] F. H. Yu, T. Wu, Z. Y. Wang, B. Lei, W. Z. Zhuo, J. J. Ying, and X. H. Chen, Concurrence of anomalous Hall effect and charge density wave in a superconducting topological kagome metal, *Phys. Rev. B* **104**, L041103 (2021).
- [34] Z. Liang, X. Hou, F. Zhang, W. Ma, P. Wu, Z. Zhang, F. Yu, J.-J. Ying, K. Jiang, L. Shan, Z. Wang, and X.-H. Chen, Three-dimensional charge density wave and surface-dependent vortex-core states in a kagome superconductor CsV₃Sb₅, *Phys. Rev. X* **11**, 031026 (2021).
- [35] Z. Wang, Y.-X. Jiang, J.-X. Yin, Y. Li, G.-Y. Wang, H.-L. Huang, S. Shao, J. Liu, P. Zhu, N. Shumiya, M. S. Hossain, H. Liu, Y. Shi, J. Duan, X. Li, G. Chang, P. Dai, Z. Ye, G. Xu, Y. Wang, H. Zheng, J. Jia, M. Z. Hasan, and Y. Yao, Electronic nature of chiral charge order in the kagome superconductor CsV₃Sb₅, *Phys. Rev. B* **104**, 075148 (2021).
- [36] M. D. Johannes and I. I. Mazin, Fermi surface nesting and the origin of charge density waves in metals, *Phys. Rev. B* **77**, 165135 (2008).
- [37] S. Barišić, J. Labbé, and J. Friedel, Tight binding and transition-metal superconductivity, *Phys. Rev. Lett.* **25**, 919 (1970).
- [38] F. Weber, S. Rosenkranz, J.-P. Castellan, R. Osborn, R. Hott, R. Heid, K.-P. Bohnen, T. Egami, A. H. Said, and D. Reznik, Extended phonon collapse and the origin of the charge-density wave in 2H - NbSe₂, *Phys. Rev. Lett.* **107**, 107403 (2011).
- [39] X. Zhu, Y. Cao, J. Zhang, E. W. Plummer, and J. Guo, Classification of charge density waves based on their nature, *Proceedings of the National Academy of Sciences* **112**, 2367 (2015).
- [40] J.-P. Pouget, E. Canadell, and B. Guster, Momentum-dependent electron-phonon coupling in charge density wave systems, *Phys. Rev. B* **103**, 115135 (2021).
- [41] J. Zaanen and O. Gunnarsson, Charged magnetic domain lines and the magnetism of high- T_c oxides, *Phys. Rev. B* **40**, 7391 (1989).
- [42] K. Machida, Magnetism in La₂CuO₄ based compounds, *Physica C: Superconductivity* **158**, 192 (1989).
- [43] D. Poilblanc and T. M. Rice, Charged solitons in the hartree-fock approximation to the large-U Hubbard model, *Phys. Rev. B* **39**, 9749 (1989).
- [44] C. M. Varma and A. L. Simons, Strong-coupling theory of charge-density-wave transitions, *Phys. Rev. Lett.* **51**, 138 (1983).
- [45] H. Li, T. T. Zhang, T. Yilmaz, Y. Y. Pai, C. E. Marvinney, A. Said, Q. W. Yin, C. S. Gong, Z. J. Tu, E. Vescovo, C. S. Nelson, R. G. Moore, S. Murakami, H. C. Lei, H. N. Lee, B. J. Lawrie, and H. Miao, Observation of unconventional charge density wave without acoustic phonon anomaly in kagome superconductors AV₃Sb₅ (A = Rb, Cs), *Phys. Rev. X* **11**, 031050 (2021).
- [46] H. Luo, Q. Gao, H. Liu, Y. Gu, D. Wu, C. Yi, J. Jia, S. Wu, X. Luo, Y. Xu, L. Zhao, Q. Wang, H. Mao, G. Liu, Z. Zhu, Y. Shi, K. Jiang, J. Hu, Z. Xu, and X. J. Zhou, Electronic nature of charge density wave and electron-phonon coupling in Kagome superconductor KV₃Sb₅ (2021), [arXiv:2107.02688 \[cond-mat.supr-con\]](#).
- [47] S. Cho, H. Ma, W. Xia, Y. Yang, Z. Liu, Z. Huang, Z. Jiang, X. Lu, J. Liu, Z. Liu, J. Jia, Y. Guo, J. Liu, and D. Shen, Emergence of new van Hove singularities in the charge density wave state of a topological kagome metal RbV₃Sb₅ (2021), [arXiv:2105.05117 \[cond-mat.supr-con\]](#).
- [48] Z. Wang, S. Ma, Y. Zhang, H. Yang, Z. Zhao, Y. Ou, Y. Zhu, S. Ni, Z. Lu, H. Chen, K. Jiang, L. Yu, Y. Zhang, X. Dong, J. Hu, H.-J. Gao, and Z. Zhao, Distinctive momentum dependent charge-density-wave gap observed in CsV₃Sb₅ superconductor with topological kagome lattice (2021), [arXiv:2104.05556 \[cond-mat.supr-con\]](#).
- [49] K. Nakayama, Y. Li, T. Kato, M. Liu, Z. Wang, T. Takahashi, Y. Yao, and T. Sato, Multiple energy scales and anisotropic energy gap in the charge-density-wave phase of kagome superconductor CsV₃Sb₅ (2021), [arXiv:2104.08042 \[cond-mat.supr-con\]](#).
- [50] Y. Xie, Y. Li, P. Bourges, A. Ivanov, Z. Ye, J.-X. Yin, M. Z. Hasan, A. Luo, Y. Yao, Z. Wang, G. Xu, and P. Dai, Electron-phonon coupling in the charge density wave state of CsV₃Sb₅ (2021), [arXiv:2111.00654 \[cond-mat.str-el\]](#).
- [51] H. Zhao, H. Li, B. R. Ortiz, S. M. L. Teicher, T. Park, M. Ye, Z. Wang, L. Balents, S. D. Wilson, and I. Zeljkovic, Cascade of correlated electron states in a kagome superconductor CsV₃Sb₅, *Nature* **10.1038/s41586-021-03946-w** (2021).
- [52] H. Chen, H. Yang, B. Hu, Z. Zhao, J. Yuan, Y. Xing, G. Qian, Z. Huang, G. Li, Y. Ye, S. Ma, S. Ni, H. Zhang, Q. Yin, C. Gong, Z. Tu, H. Lei, H. Tan, S. Zhou, C. Shen, X. Dong, B. Yan, Z. Wang, and H.-J. Gao, Roton pair density wave in a strong-coupling kagome superconductor, *Nature* **10.1038/s41586-021-03983-5** (2021).
- [53] H. Li, Y.-X. Jiang, J. X. Yin, S. Yoon, A. R. Lupini, Y. Pai, C. Nelson, A. Said, Y. M. Yang, Q. W. Yin, C. S. Gong, Z. J. Tu, H. C. Lei, B. Yan, Z. Wang, M. Z. Hasan, H. N. Lee, and H. Miao, Spatial symmetry constraint of charge-ordered kagome superconductor CsV₃Sb₅ (2021), [arXiv:2109.03418 \[cond-mat.mtrl-sci\]](#).
- [54] L. Yu, C. Wang, Y. Zhang, M. Sander, S. Ni, Z. Lu, S. Ma, Z. Wang, Z. Zhao, H. Chen, K. Jiang, Y. Zhang, H. Yang, F. Zhou, X. Dong, S. L. Johnson, M. J. Graf, J. Hu, H.-J. Gao, and Z. Zhao, Evidence of a hidden flux phase in the topological kagome metal CsV₃Sb₅ (2021), [arXiv:2107.10714 \[cond-mat.supr-con\]](#).
- [55] G. Kresse and J. Furthmüller, Efficient iterative schemes for ab initio total-energy calculations using a plane-wave basis set, *Phys. Rev. B* **54**, 11169 (1996).
- [56] G. Kresse and J. Hafner, Ab initio molecular dynamics for open-shell transition metals, *Phys. Rev. B* **48**, 131115 (1993).
- [57] G. Kresse and D. Joubert, From ultrasoft pseudopotentials to the projector augmented-wave method, *Phys. Rev. B* **59**, 1758 (1999).
- [58] J. P. Perdew, K. Burke, and M. Ernzerhof, Generalized gradient approximation made simple, *Phys. Rev. Lett.*

- 77**, 3865 (1996).
- [59] A. A. Mostofi, J. R. Yates, G. Pizzi, Y.-S. Lee, I. Souza, D. Vanderbilt, and N. Marzari, An updated version of wannier90: A tool for obtaining maximally-localised wannier functions, *Computer Physics Communications* **185**, 2309 (2014).
 - [60] Q. Wu, S. Zhang, H.-F. Song, M. Troyer, and A. A. Soluyanov, Wanniertools: An open-source software package for novel topological materials, *Computer Physics Communications* **224**, 405 (2018).
 - [61] D. W. Song, L. X. Zheng, F. H. Yu, J. Li, L. P. Nie, M. Shan, D. Zhao, S. J. Li, B. L. Kang, Z. M. Wu, Y. B. Zhou, K. L. Sun, K. Liu, X. G. Luo, Z. Y. Wang, J. J. Ying, X. G. Wan, T. Wu, and X. H. Chen, Orbital ordering and fluctuations in a kagome superconductor CsV_3Sb_5 (2021), [arXiv:2104.09173 \[cond-mat.supr-con\]](#).
 - [62] C. M. I. au2, D. Das, J. X. Yin, H. Liu, R. Gupta, C. N. Wang, Y. X. Jiang, M. Medarde, X. Wu, H. C. Lei, J. J. Chang, P. Dai, Q. Si, H. Miao, R. Thomale, T. Neupert, Y. Shi, R. Khasanov, M. Z. Hasan, H. Luetkens, and Z. Guguchia, Time-reversal symmetry-breaking charge order in a correlated kagome superconductor (2021), [arXiv:2106.13443 \[cond-mat.mtrl-sci\]](#).
 - [63] N. Shumiya, M. S. Hossain, J.-X. Yin, Y.-X. Jiang, B. R. Ortiz, H. Liu, Y. Shi, Q. Yin, H. Lei, S. S. Zhang, G. Chang, Q. Zhang, T. A. Cochran, D. Multer, M. Litskevich, Z.-J. Cheng, X. P. Yang, Z. Guguchia, S. D. Wilson, and M. Z. Hasan, Intrinsic nature of chiral charge order in the kagome superconductor Rbv_3sb_5 , *Phys. Rev. B* **104**, 035131 (2021).
 - [64] E. M. Kenney, B. R. Ortiz, C. Wang, S. D. Wilson, and M. Graf, Absence of local moments in the kagome metal KV_3Sb_5 as determined by muon spin spectroscopy, *Journal of Physics: Condensed Matter* (2021).
 - [65] D. Wu, Q. M. Liu, S. L. Chen, G. Y. Zhong, J. Su, L. Y. Shi, L. Tong, G. Xu, P. Gao, and N. L. Wang, Layered semiconductor EuTe_4 with charge density wave order in square tellurium sheets, *Phys. Rev. Materials* **3**, 024002 (2019).
 - [66] M. Perrot, P. Delplace, and A. Venaille, Topological transition in stratified fluids, *Nature Physics* **15**, 781 (2019).